J Nanopart Res (2013) 15:1447
DOI 10.1007/s11051-013-1447-2

RESEARCH PAPER

Kinetics of dissolution of a biocide soda-lime glass powder containing silver nanoparticles

L. Esteban-Tejeda · A. C. da Silva · S. R. Mello-Castanho · C. Pacharroman · J. S. Moya

Received: 28 November 2012 / Accepted: 17 January 2013 / Published online: 31 January 2013

Abstract In the present study we have studied the lixiviation kinetics of silver nanoparticles, as well as the solubility of a particulate system (<30 μm) composed of a glassy matrix of soda-lime glass containing 20 wt% of silver nanoparticles, under a constant flow (0.21 l/day) of deionizated water at room temperature. The kinetic of silver, CaO and SiO_2 lixiviation followed a Jander model ($\alpha^2/4 \approx Kt$). It has been proven that nanostructured soda-lime glass/nAg composed by particles <30 μm with a 20 wt% of silver are a strong biocide versus Gram-positive, Gram-negative bacteria and yeasts. This soda-lime glass/nAg acts as a perfect dispenser of silver nanoparticles to the liquid media, avoiding the fast increasing of its concentration over the toxicity limit for human cells and for the environment.

Keywords Jander model · Low toxicity · Glass-nAg · Biocide

L. Esteban-Tejeda (✉) · C. Pacharroman · J. S. Moya
Department of Biomaterials and Bioinspired Materials, Materials Science Institute of Madrid (ICMM-CSIC), Cantoblanco, 28049 Madrid, Spain
e-mail: lesteban@icmm.csic.es

A. C. da Silva · S. R. Mello-Castanho
Energy and Nuclear Research Institute (IPEN), Sao Paulo, Brazil

Introduction

The development of nanotechnology has involved the use of silver nanoparticles in laboratories as well as in consumer products. However, these nanoparticles present health and environment problems because of their small size and high reactivity (Dockery et al. 1993; Seaton et al. 2009). Nanoparticles can be easily introduced in the human body through the lungs, the skin or the gastrointestinal tract. Once introduced in the body, they can be incorporated to the bloodstream, the lymphatic system and the nervous system reaching organs and tissues, such as the brain, disrupting their correct operation (Gopinath et al. 2008; Oberdörster et al. 2004; Panyala et al. 2008; Takenaka et al. 2001). The effects of silver nanoparticles on the environment are related to the toxic influence on the beneficial bacteria in soil, which play an important role in the nitrogen fixation, in the delivering of many essential nutrients to the soil formation or in the organic matter decomposition (Murata et al. 2005; Panyala et al. 2008). These problems can be solved using a matrix to embed the silver nanoparticles. A glassy matrix is the best option, because it is possible to design the glass composition depending on the application required. With this, the releasing of nanoparticles to the media can be controlled by the partial dissolution of the glassy matrix. This turns the glass into a dispenser of silver nanoparticles, avoiding the health and environmental problems. In addition, this material is focused to be used as a biocide due to the known antibacterial

and antifungal properties of the silver nanoparticles (Gogoi et al. 2006; Lu et al. 2008; Marambio-Jones et al. 2010; Rai et al. 2009; Sondi et al. 2004; Yoon et al. 2007). Because of this, the controlled releasing of silver nanoparticles is highly important, in order to dose the nanoparticles and keep the biocide activity for a long time without toxicity. The aim of this study is the development of a new antimicrobial agent free of toxicity due to the dosage of nanoparticles. We have chosen as a matrix a soda-lime glass because of its suitable solubility. The glassy matrix is gradually dissolved and then, releases the silver nanoparticles to the media. In the present study, we have studied the lixiviation of theses silver nanoparticles as well as the solubility of the glassy matrix.

Experimental

Materials

As source of nanoparticles the vitellinate/nAg (Batch n° 127, ARGENOL S.L.), which is a protein of high molecular weight with a particle size distribution of $d_{50} \approx 10 \pm 2$ nm was selected. This sample was fully characterized in a previous work (Esteban-Tejeda et al. 2010) by differential thermal analysis (DTA), thermogravimetry (TG), X-Ray diffraction (XRD), ultraviolet–visible absorption spectroscopy (UV–VIS spectroscopy) and transmission electron microscopy (TEM). The chemical analysis of the vitellinate/nAg was determined by inductively coupled plasma (ICP) (Thermo Jarrell Ash IRIS ADVANTAGE) and was found to be 20 wt% of silver and 7.6 wt% of sodium oxide. As matrix to embed the silver nanoparticles a commercial soda-lime glass from the SiO_2–Na_2O–K_2O–CaO–MgO–B_2O_3 system with the following chemical composition (wt%): 70.2 SiO_2, 15.8 Na_2O, 7.1 CaO, 3.2 MgO 1.06, B_2O_3 and 0.05 K_2O with a deformation point $\sim$668 °C was used.

Synthesis of glass/nAg powder

The glass was milled to <30 μm in a planetary agate ball mill and mixed in isopropyl alcohol with the corresponding fraction of nAg/vitellinate to obtain a glass/nAg with 20 wt% of silver under constant stirring of 30 rpm. After drying at 60 °C for 4 h, the homogeneous mixture was uniaxially pressed at 250 MPa into pellets (10 mm diameter). Afterwards, they were sintered in air, in two-steps by heating at a rate of 3 °C/min to 500, 725 °C, respectively, and holding for 1 h. Tubular electrical furnace and zirconia crucibles were used. The obtained glass/nAg pellets were milled down to <30 μm in a planetary agate ball mill. These powders were fully characterized by XRD using a Bruker D8 diffractometer using CuKα radiation working at 40 kV and 30 mA in a step-scanning mode from 10 to 70° with a step width of 0.0288 and a step time of 2.5 s and by transmission electron microscopy (TEM) (JEOL FXII at 200 kV). Optical absorption spectrum was measured in a range from 200 to 800 nm, using a JASCO UV–Vis V-660 spectrophotometer to determine the surface plasmon resonance of silver nanoparticles. The particle size of the glass/nAg was also determined using a MASTERSIZER model 2.18.

Biocide test

The antimicrobial activity of the glass/nAg powder (20 wt%) was evaluated against three different microorganisms: *Escherichia coli JM110* (Gram-negative bacteria), *Micrococcus luteus* (Gram-positive bacteria) and *Issatchenkia orientalis* (yeast).

Hydrolytic resistance test

The hydrolytic resistance of the glass/nAg powder (20 wt%) was carried out using the method described by Fagerlund (Fagerlund et al. 2012). 1 g of the glass/nAg powder (20 wt%) was deposited on filter paper, and a constant flow (0.21 l/day) of deionizated water at room temperature (25 °C) was passed through during 60 days. Finally, this water was collected in a container. Every day an aliquot was removed to be determined by ICP (ICP Perkin Elmer mod. optima 2,100 DV) the fractions of silver, calcium and silicon lixiviated from the glass.

Results and discussion

The particle size distribution of the glass/nAg (20 wt%) powder (left) and the SEM micrograph (right) are

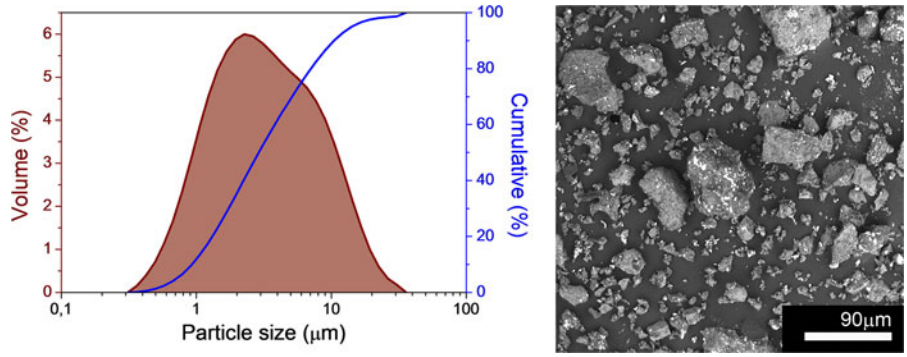

Fig. 1 Particle size distribution of the glass/nAg powder (20 wt%) (*left*) and the SEM micrograph (*right*)

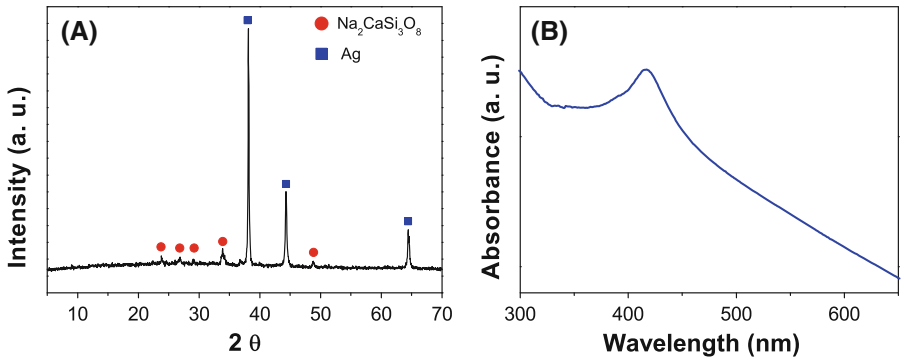

Fig. 2 XRD **a** and absorption spectrum **b** of the glass/nAg (20 wt%) powder

shown in Fig. 1. The powder is constituted by pseudo equiaxial polyhedral grains with an average particle size of 2.2 ± 0.2 μm. The XRD pattern of the powder exhibits the peaks corresponding to silver and precipitates of a sodium calcium silicate ($Na_2CaSi_3O_8$). The UV–Vis spectrum shows a broad peak at about 410 nm corresponding to silver nanoparticles (Fig. 2).

Biocide test

The logarithm reduction was used to characterize the effectiveness of the glass/nAg (20 wt%) powder. The logarithm reduction was calculated as follows:

$$\text{Logarithm reduction} = \log A - \log B \quad (1)$$

where A is the average number of viable cells from inoculum control (microorganisms and nutrients without biocide agent) after 24 h, and B is the average number of viable cells from the culture with the glass/nAg after 24 h.

In Fig. 3 the biocide activity for the glass/nAg (20 wt%) powder against *Escherichia coli JM110*, *Micrococcus luteus* and *Issatchenkia orientalis* is plotted. From the three microorganisms studied, the logarithm reduction was found to be higher than 4, which means a complete disinfection.

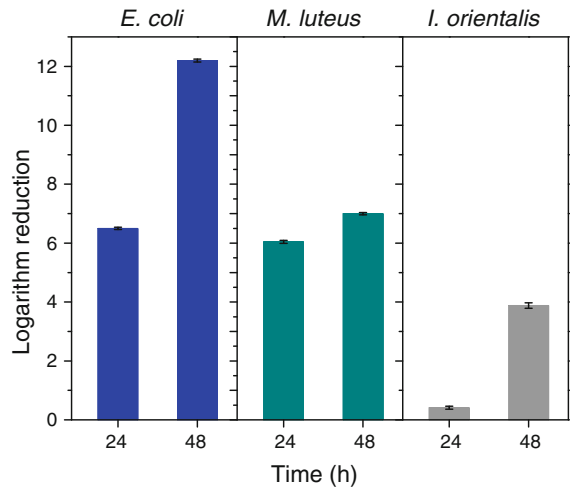

Fig. 3 Logarithm reduction for the glass/nAg (2.6wt%) against: *E. coli*, *M. luteus* and *I. orientalis*. The data obtained for glass/nAg (>2.6wt%) samples were found to be very similar to these ones

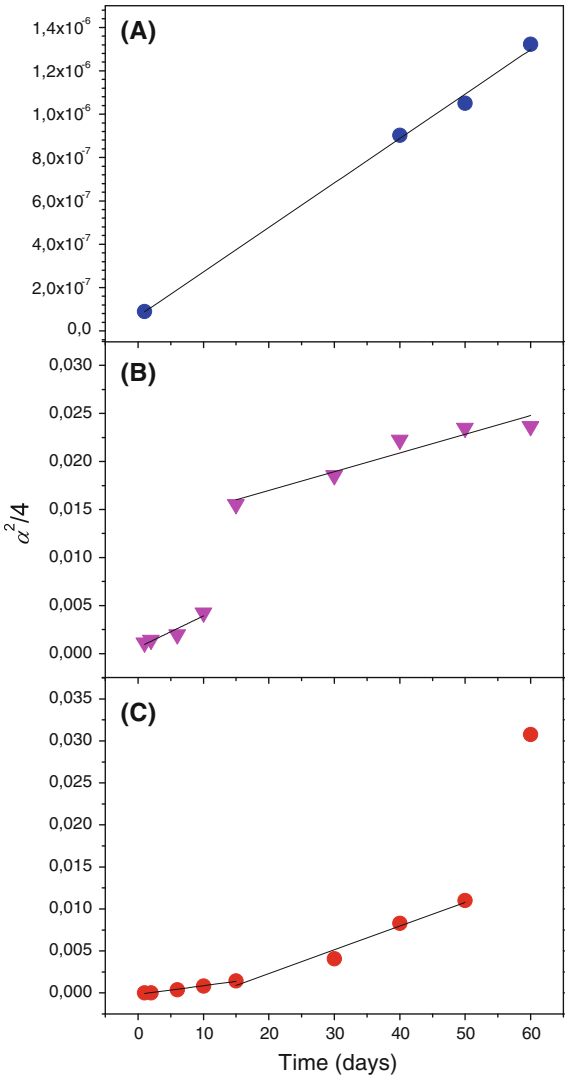

Fig. 4 Fraction lixiviated from the glass/nAg (20 wt%) during 60 days of hydrolytic study of silver (**a**), silica (**b**) and calcium (**c**)

Hydrolytic resistance

The corresponding fractions of silver, calcium and silicon lixiviated from the glass/nAg (20 wt%) powder are plotted in Fig. 4. The glass/nAg (20 wt%) powder was also analyzed by transmission electron microscopy (JEOL FXII at 200 kV) before (Fig. 5) and after (Fig. 6) the hydrolytic attack.

The microstructure of the glass/nAg (20 wt%) powder before and after the hydrolytic attack was also evaluated. After the hydrolytic attack this powder shows a more angular outline than the glass/nAg (20 wt%) before due to the loss of part of the glassy structure, mainly the tetrahedral SiO_2. However, after the hydrolytic attack, a great amount of silver nanoparticles were kept in the glassy matrix as it is shown in Fig. 6. This is in good agreement with the lixiviation study represented in Fig. 4. As it can be inferred from these analyses, the glassy/nAg (20 wt%) particles are hydrolytically attacked following a mechanism similar to the one described by Mello-Castanho et al. (Mello-Castanho et al. 2006; Silva et al. 2004, 2007) for soda-lime glasses. In agreement with this mechanism, the alkaline and alkaline earth elements are first lixiviated forming a superficial silica rich layer. This layer is constituted by amorphous silica so it has no structural character and may contribute to improve both the glass resistance and the pH solution stabilization. According to some authors, (Koenderink 2000; Navarro 1991; Sigoli 2001) the presence of this layer is an indicative that the dissolution of the glass is attained by the alkalis extraction and by the hydrolyses of the Si–O bonds process. Afterwards, this layer is detached by this process becoming continuous to lixiviate the silver nanoparticles (3–20 nm) slowly and gradually.

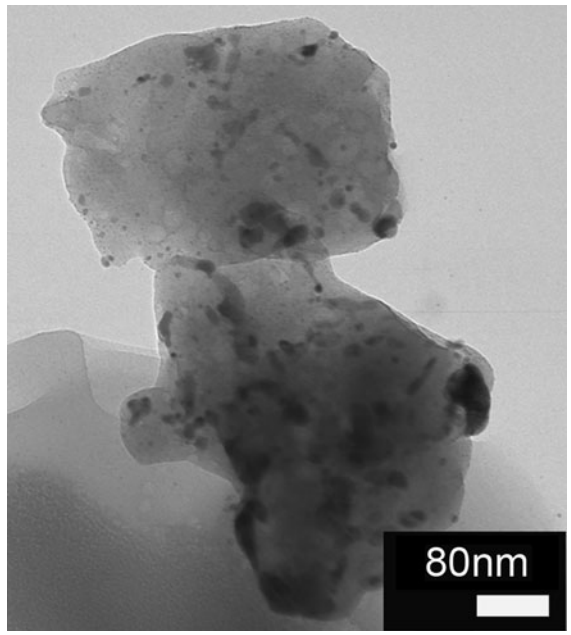

Fig. 5 TEM micrographs of the glass/nAg (20 wt%) powder before the hydrolytic attack

According to Jander equation which is operating in the case of reactions controlled by diffusion, the following expressions can be deduced:

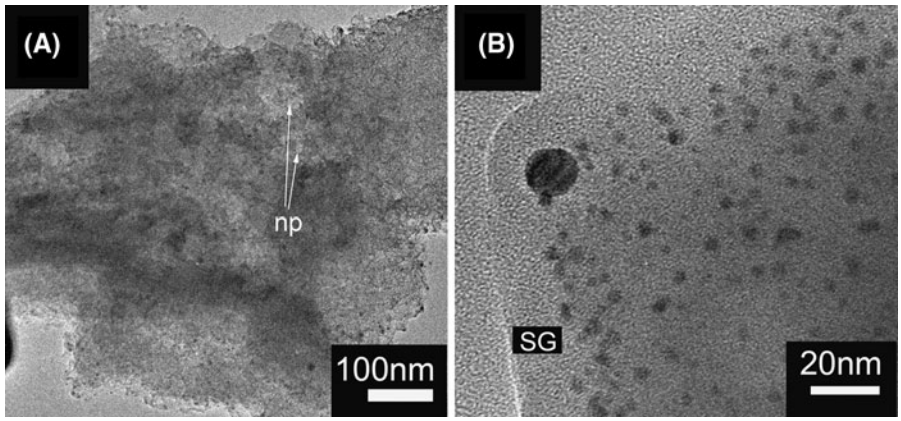

Fig. 6 TEM micrographs of the glass/nAg (20 wt%) powder after 60 days of the hydrolytic attack. SG: Silica glass and np: nanopores

$$\left\{1-(1-\alpha)^{1/2}\right\}^2 = \mathrm{Kt} \qquad (2)$$

If $\alpha \ll 1$, as in our case,

$$(1-\alpha)^{1/2} \approx 1-\alpha/2$$

$$(1-1-\alpha/2)^2 \approx \alpha^2/4$$

$$\alpha^2/4 \approx \mathrm{Kt}$$

From Fig. 4, the presence of a break point is clear at about 15 days of water dissolution of SiO_2 and CaO. This fact can be rationalized considering the detachment of the already formed silica rich layer (Mello-Castanho et al. 2006). Then, the dissolution process will start again from the new glass surface. That is, the dissolution of the glassy matrix is a discontinuous process which decreases/retards the lixiviation rate of the silver nanoparticles. These nanoparticles are delivered to the liquid media mainly after the detachment of the silica reach layer (Fig. 6). This fact explains the observed increases in the content of silver after 60 days of treatment as well as the open nanopores morphology of the glass particles surface detected by TEM analysis (Fig. 6). No oxidation of silver nanoparticles was observed in this particular case, probably due to the fact that these nanoparticles are embedded in the glassy matrix and not in direct contact with a moist atmosphere (Lavrenko et al. 2006).

Conclusions

We can conclude that this particulate system (<30 μm) composed of a glassy matrix of soda-lime glass containing 20wt % of silver nanoparticles, acts as a perfect dispenser of silver nanoparticles to the water media avoiding the fast increasing of its concentration over the toxicity limit of 30 ppm for human fibroblasts (Panacek et al. 2009), as well as versus the environment. In the conditions of our experiments the concentration of silver nanoparticles was found to be <1 ppm. This nanostructured powder has been proven to be a strong biocide versus Gram-positive bacteria, Gram-negative bacteria and yeasts.

Acknowledgments This study has been supported by CSIC project reference number 20136E012, the Spanish Ministry of Science and Innovation (MICINN) under the project MAT2012-38645 and IPEN, Sao Paulo, Brazil.

References

Dockery DW et al (1993) An association between air pollution and mortality in six US cities. N Engl J Med 329(24): 1753–1759

Esteban-Tejeda L, Malpartida F, Pecharroman C, Moya JS (2010) High antibacterial and antifungal activity of silver monodispersed nanoparticles embedded in a glassy matrix. Adv Eng Mater 12(7):B292–B297

Fagerlund S, Ek P, Hupa L, Hupa M (2012) Dissolution kinetics of a bioactive glass by continuous measurement. J Am Ceram Soc 95:3130–3137

Gogoi SK et al (2006) Green fluorescent protein-expressing *Escherichia coli* as a model system for investigating the antimicrobial activities of silver nanoparticles. Langmuir 22(22):9322–9328

Gopinath P, Gogoi SK, Chattopadhyay A, Ghosh SS (2008) Implications of silver nanoparticle induced cell apoptosis for in vitro gene therapy. Nanotechnology 19(7):075104

Koenderink GH (2000) Effect of the initial stages of leaching on the surface of alkaline earth sodium silicate glasses. J Non-Cryst Solids 262(1–3):80–98

Lavrenko VA et al (2006) Features of hih-temperature oxidation in air of silver and alloy Ag-Cu, and adsorption of oxygen on silver. Powder Metall Met Ceram 45(9–10):476–480

Lu L et al (2008) Silver nanoparticles inhibit hepatitis B virus replication. Antivir Therapy 13(2):252–262

Marambio-Jones C, Hoek E (2010) A review of the antibacterial effects of silver nanomaterials and potential implications for human health and the environment. J Nanopar Res 12(5): 1531–1551

Mello-Castanho SRH et al (2006) Vidrios de silicato a partir de residuos galvánicos con alto contenido en Cr y Ni. Bol Soc Esp Ceram Vidrio 45(1):52–57

Murata T, FKanao-koshikawa M, Takamatsu T (2005) Effects of Pb, Cu, Sb, In and Ag contamination on the proliferation of soil bacterial colonies, soil dehydrogenase activity, and phospholipid fatty acid profiles of soil microbial communities. Water Air Soil Pollut 164:103–118

Navarro JMF (1991) El vidrio. Consejo Superior de Investigaciones Científicas, Madrid

Oberdörster G et al (2004) Translocation of inhaled ultrafine particles to the brain. Inhalation Toxicol 16(6–7):437–445

Panacek A et al (2009) Antifungal activity of silver nanoparticles against *Candida spp*. Biomaterials 30(31):6333–6340

Panyala NR, Pena-Mendez EM, Havel J (2008) Silver or silver nanoparticles: a hazardous threat to the environment and human health? J Appl Biomed 6(3):117–129

Rai M, Yadav A, Gade A (2009) Silver nanoparticles as a new generation of antimicrobials. Biotechnol Adv 27(1):76–83

Seaton A, Tran L, Aitken R, Donaldson K (2009) Nanoparticles, human health hazard and regulation. J R Soc Interface. doi: 10.1098/rsif.2009.0252.focus

Sigoli FA (2001) Phase separation in pyrex glass by hydrothermal treatment: evidence from micro-Raman spectroscopy. J Non-Cryst Solids 284(1–3):49–54

Silva A, Castanho S (2004) Silicate glasses obtained from fine silica powder modified with galvanic waste addition. J Non-Cryst Solids 348:211–217

Silva AC, Mello-Castanho SRH (2007) Vitrified galvanic waste chemical stability. J Eur Ceram Soc 27(3):565–570

Sondi I, Salopek-Sondi B (2004) Silver nanoparticles as antimicrobial agent: a case study on *E. coli* as a model for Gram-negative bacteria. J Colloid Interface Sci 275(1): 177–182

Takenaka S et al (2001) Pulmonary and systemic distribution of inhaled ultrafine silver particles in rats. Environ Health Perspect 109(Suppl. 4):547–551

Yoon KY, Byeon JH, Park JH, wang JH (2007) Susceptibility constants of *Escherichia coli* and *Bacillus subtilis* to silver and copper nanoparticles. Sci Total Environ 373(2–3): 572–575